厚生労働科学研究費補助金

萌芽的先端医療技術推進研究事業

細胞内動態制御機能を有する新規細胞選択型ナノ遺伝子キャリアの開発と遺伝子治療への応用

平成１８年度　総括研究年度終了報告書

主任研究者　　川上　茂

平成１９（２００７）年　４月

目　　次

厚生労働科学研究費補助金（萌芽的先端医療技術推進研究事業）
研究報告書

細胞内動態制御機能を有する新規細胞選択型ナノ遺伝子キャリアの開発と遺伝子治療への応用

主任研究者　川上　茂　京都大学大学院薬学研究科

研究要旨　本研究は、生体内で細胞特異的デリバリーなど高度な機能を発揮する多機能性標的指向型ナノ・遺伝子キャリアの創製を行うため、細胞特異的認識素子の表面導入、あるいは細胞内動態制御の指針となる総合的な設計戦略を確立し、同時に実用性の高い *in vivo* レベル遺伝子発現制御技術の開発を目指す。さらに本研究を通して開発した新規多機能性標的指向型ナノ・遺伝子キャリアを遺伝子治療へと応用する。平成16－17年度における検討を通じて、各肝臓構成細胞が有する固有で比較的厳密な基質認識性を示す糖鎖認識機構を利用できるよう分子設計した各種糖修飾カチオン性リポソームを開発した。物理化学的性質、体内動態、遺伝子導入、毒性に関する評価を通じて基本的な細胞選択的 *in vivo* 遺伝子ターゲティングシステムの確立に成功した。一方、遺伝子治療への応用を考えていく上では、*in vivo* での導入活性のみならず治療効果との相関などを議論する必要がある。平成17年度における検討では、樹状細胞への遺伝子ターゲティングをDNAワクチン療法へ応用し、遺伝子を用いて導入したがん抗原特異的細胞障害性 T 細胞の誘導による新規がん遺伝子治療法開発に成功した。平成18年度は、本システムの核酸医薬品への遺伝子治療への応用を試みるため、炎症関連遺伝子群の発現を誘導する転写因子 NFκB に対するデコイ型 2 本鎖オリゴヌクレオチド (NFκB デコイ) を用いた新規抗炎症療法に関する評価をおこなった。その結果、細胞内動態制御機能を有するフコース修飾カチオン性リポソームでは、静脈内投与後、NFκB デコイが i) Kupffer 細胞にレセプター介在性エンドサイトーシスで細胞選択的に取り込まれ、ii) エンドソームからの脱出により効果的に NFκB 活性化を阻害し、LPS 誘発性肝疾患マウスにおける肝炎抑制効果を得ることに成功した。これらの知見は NFκB を標的とした炎症性疾患や免疫疾患に対する治療の実現に向けて有用な基礎的知見を与える。

A.　研究目的

平成 16－17 年度における検討を通じて、各肝臓構成細胞が有する固有で比較的厳密な基質認識性を示す糖鎖認識機構を利用できるよう分子設計した各種糖修飾カチオン性リポソームを開発した。物理化学的性質、体内動態、遺伝子導入、毒性に関する評価を通じて基本的な細胞選択的 *in vivo* 遺伝子ターゲティングシステムの確立に成功した。さらに、遺伝子のみならず siRNA を用いた細胞選択的な遺伝子発現抑制にも応用可能であることを報告した。一方、遺伝子治療への応用を考えていく上では、*in vivo* での導入活性のみならず治療効果との相関などを議論する必要がある。そこで平成 17 年度における検討では、樹状細胞への遺伝子ターゲティングを DNA ワクチン療法へ応用し、遺伝子を用いて導入したがん抗原特異的細胞障害性 T 細胞の誘導による新規がん遺伝子治療法開発に成功した。

平成 18 年度は、本システムの核酸医薬品への遺伝子治療への応用を試みるため、炎症関連遺伝子群の発現を誘導する転写因子 NFκB に対するデコイ型 2 本鎖オリゴヌクレオチド (NFκB デコイ) を用いた新規抗炎症療法に関する評価をおこなった。

B. 研究方法

リポソームの調製: Man-C4-Chol/DOPE をモル比 3:2 の割合で混合し、vortex 法により調製した。物理化学的性質の測定:ゼータ電位および平均粒子径は動的光散乱法により測定した。*In vivo* 体内動態の評価: 蛍光あるいは[^{32}P]標識 NFκB デコイを調製した。5 週齢雌性 ICR マウス（22 – 25 g）の静脈内へ各種複合体を投与した。マウスを安楽死させ、肝臓、肺、心臓、脾臓、腎臓への移行を組織切片あるいは放射活性により評価した。薬理効果の評価：LPS 誘発性肝炎を

誘発させ、複合体による抑制効果を肝臓中NFkB 量、血清中サイトカイン、aspartate aminotransferase (AST) 、 alanine aminotransferase (ALT)の測定を指標に行った。

C.D. 結果・考察

Fuc-C4-Chol, DOPE により細胞内動態制御機能を有するフコース修飾カチオン性リポソーム (Fuc リポソーム) を調製した。初代培養 Kupffer 細胞を用いて Fuc リポソーム/[^{32}P]標識 NFκB デコイ複合体の細胞への取り込みを評価した結果、対照の naked NFκB デコイおよびカチオン性リポソーム複合体より高い細胞取り込みが認められた。競合阻害実験により、リポソーム複合体がフコースレセプターにより取り込まれていることが示唆された。

In vivo において Fuc リポソーム/NFκB デコイ複合体の静脈内投与による Kupffer 細胞選択的な送達および炎症抑制効果について検討した。静脈内投与後、Fuc リポソーム/[^{32}P]標識 NFκB デコイ複合体は、対照の naked NFκB デコイおよびカチオン性リポソーム複合体に比べ、有意に高く肝臓へ集積した。また、肝臓内細胞分布に関しては、Kupffer 細胞が存在する肝非実質細胞への集積が認められた。さらに、Kupffer 細胞に障害を与える $GdCl_3$ を前投与したところ、Fuc リポソーム/NFκB デコイ複合体の肝臓への集積が有意に減少し、Kupffer 細胞での高い取り込みが示唆された。

LPS 誘発性肝疾患マウスに対し、Fuc リポソーム/NFκB デコイ複合体を静脈内投与したところ、対照の naked NFκB デコイ、カチオン性リポソーム複合体と比べ、血清中 TNFα量、IFNγ量の有意な抑制効果が認められた。また、本治療実験に用いたマウス肝臓核内 NFκB 量を評価したところ、有意な核内 NFκB 量の増加抑制が認められ、Fuc リポソーム/NFκB デコイ複合体による NFκB の活性化抑制が確認された。さらに、Fuc リポソーム/NFκB デコイ複合体による AST、ALT の有意な抑制も認められ、肝炎治療の可能性が強く示唆された。

E. 結論

細胞内動態制御機能を有する Fuc リポソームにより、NFκB デコイの静脈内投与による Kupffer 細胞選択的な送達を実現し、LPS 誘発性肝疾患マウスにおける TNFαの産生抑制効果を得ることに成功した。以上の知見は、NFκB を標的とした炎症性疾患や免疫疾患に対する治療の実現に向けて有用な基礎的知見を与える。

F. 健康危険情報

なし

G. 研究発表

1. 論文発表

1. T. Terada, M. Mizobata, **S. Kawakami**, F. Yamashita, and M. Hashida: Optimization of tumor-selective targeting by basic fibroblast growth factor-binding peptide grafted PEGylated liposomes,
Journal of Controlled Release, in press (2007)

2. K. Shigeta, **S. Kawakami**, Y. Higuchi, T. Okuda, H. Yagi, F. Yamashita, and M. Hashida: Novel histidine-conjugated galactosylated cationic liposomes for efficient hepatocyte-selective gene transfer in human hepatoma HepG2 cells,
Journal of Controlled Release, 118, (2), 262-270 (2007)

3. A. Sato, M. Takagi, A. Shimamoto, **S. Kawakami**, M. Hashida: Small interfering RNA delivery to the liver by intravenous administration with galactosylated cationic liposomes,
Biomaterials, 28 (7), 1434-1442 (2007)

4. Y. Higuchi, **S. Kawakami**, F. Yamashita, M. Hashida: The potential role of fucosylated cationic liposome/NFkB decoy complexes in the treatment of cytokine-related liver disease,
Biomaterials, 28 (3), 532-539 (2007)

5. T. Okuda, **S. Kawakami**, N. Akimoto, T. Niidome, F. Yamashita, M. Hashida: PEGylated dendritic poly(L-lysine)s for tumor-selective targeting following the intravenous injection in mice,
Journal of Controlled Release, 116(3), 330-336 (2006)

6. Y. Saito, **S. Kawakami**, Y. Yabe, F. Yamashita, M. Hashida: Intracellular trafficking is the important process that determines the optimal charge ratio on transfection by galactosylated lipoplex in HepG2 cells,
Biological & Pharmaceutical Bulletin, 29(9), 1986-1990 (2006)

7. T. Terada, M. Mizobata, **S. Kawakami**, Y. Yabe, F. Yamashita, M. Hashida: Basic fibroblast growth factor-binding peptide as a novel targeting ligand of drug carrier to tumor cells,
Journal of Drug Targeting, 14 (8), 536-545 (2006)
8. W. Yeeprae, **S. Kawakami**, F. Yamashita, M. Hashida: Effect of mannose density on mannose receptor-mediated cellular uptake of mannosylated O/W emulsions by macrophages,
Journal of Controlled Release, 114 (2), 193-201 (2006)
9. Y. Hattori, **S. Kawakami**, K. Nakamura, F. Yamashita, M. Hashida: Efficient gene transfer into macrophages and dendritic cells by in vivo gene delivery with mannosylated lipoplex via intraperitoneal route,
Journal of Pharmacology and Experimental Therapeutics, 318 (2), 828-834 (2006)
10. T. Okuda, **S. Kawakami**, T. Maeie, T. Niidome, F. Yamashita, M. Hashida: Biodistribution characteristics of amino acid dendrimers and its PEGylated derivative after intravenous administration,
Journal of Controlled Release, 114 (1), 69-77 (2006)
11. Y. Higuchi, **S. Kawakami**, S. Fumoto, F. Yamashita, M. Hashida: Effect of particle size of galactosylated lipoplex on hepatocyte-selective gene transfection after intraportal administration,
Biological & Pharmaceutical Bulletin, 29 (7), 1521-1523 (2006)
12. M. Teshima, **S. Kawakami**, S. Fumoto, K. Nishida, J. Nakamura, M. Nakashima, H. Nakagawa, N. Ichikawa, H. Sasaki: PEGylated liposomes loading palmitoyl prednisolone for prolonged blood concentration of prednisolone,
Biological & Pharmaceutical Bulletin, 29 (7), 1436-1440 (2006)
13. Y. Higuchi, **S. Kawakami**, M. Oka, Y. Yabe, F. Yamashita, M. Hashida: Intravenous administration of mannosylated cationic liposome/NFκB decoy complexes effectively prevent LPS-induced cytokine production in a murine liver failure model,
FEBS Letters, 580 (15), 3707-3714 (2006)
14. Y. Hattori, **S. Kawakami**, Y. Lu, K. Nakamura, F. Yamashita, M. Hashida: Enhanced DNA vaccine potency by mannosylated lipoplex after intraperitoneal administration,
Journal of Gene Medicine, 8 (7), 824-834 (2006)
15. **S. Kawakami**, Y. Ito, P. Charoensit, F. Yamashita, M. Hashida: Evaluation of proinflammatory cytokine production induced by linear and branched polyethylenimine/plasmid DNA complexes in mice,
Journal of Pharmacology and Experimental Therapeutics, 317 (3), 1382-1390 (2006)
16. T. Terada, M. Iwai, **S. Kawakami**, F. Yamashita, M. Hashida: Novel PEG-matrix metalloproteinase-2 cleavable peptide-lipid containing galactosylated liposomes for hepatocellular carcinoma-selective targeting,
Journal of Controlled Release, 111 (3), 333-342 (2006)
17. Y. Higuchi, **S. Kawakami**, M. Oka, F. Yamashita, M. Hashida: Suppression of TNF(production in LPS induced liver failure mice after intravenous injection of cationic liposomes/NFκB decoy complex,
Pharmazie, 61 (2), 144-147 (2006)

2. 学会発表

1. 川上 茂、橋田 充：細胞選択的遺伝子ターゲティングシステムの開発と遺伝子治療への応用、第 22 回日本 DDS 学会、日本 DDS 学会、2006 年 7 月 7 日、東京
2. 川上 茂：薬物および遺伝子ターゲティングを目的とした DDS キャリアの開発、第 21 回生物薬剤学サマーセミナー、2006 年 8 月 7 日、京都
3. 川上 茂：細胞選択的遺伝子ターゲティングを目的とした糖修飾リポソームの開発に関する研究、第 8 回製剤研究フォーラム、万有生命科学振興財団、2006 年 9 月 15 日、京都
4. 川上 茂、橋田 充：樹状細胞選択的遺伝子送達キャリアを用いた新規 DNA ワクチン療法の開発、第 65 回日本癌学会総会、日本癌学会、2006 年 9 月 29 日、横浜
5. 川上 茂：糖修飾リポソームによる細胞選択的遺伝子ターゲティングシステムの開発、第 21 回日本薬物動態学会年会、2006 年 11 月 30 日、東京
6. 川上 茂：細胞選択的ターゲティングを目的とした糖修飾リポソームの開発と遺伝子治療への応用、日本薬学会第 127 年会、2007 年 3 月 28 日

2. 実用新案登録 なし
3. その他 なし

雑誌

発表者氏名	論文タイトル名	発表誌名	巻号	ページ	出版年
T. Terada M. Mizobata S. Kawakami F. Yamashita M. Hashida	Optimization of tumor-selective targeting by basic fibroblast growth factor-binding peptide grafted PEGylated liposomes	Journal of Controlled Release		in press	
Y. Higuchi S. Kawakami F. Yamashita M. Hashida	The potential role of fucosylated cationic liposome/NFkB decoy complexes in the treatment of cytokine-related liver disease	Biomaterials	28(3)	532-539	2007
A. Sato M. Takagi A. Shimamoto S. Kawakami M. Hashida	Small interfering RNA delivery to the liver by intravenous administration of galactosylated cationic liposomes in mice	Biomaterials	28(7)	1434-1442	2007
T. Okuda S. Kawakami N. Akimoto T. Niidome F. Yamashita M. Hashida	PEGylated lysine dendrimers for tumor-selective targeting after intravenous injection in tumor-bearing mice	Journal of Controlled Release	116(3)	330-336	2006
Y. Saito S. Kawakami Y. Yabe F. Yamashita M. Hashida	Intracellular trafficking is the important process that determines the optimal charge ratio on transfection by galactosylated lipoplex in HepG2 cells	Biological and Pharmaceutical Bulletin	29(9)	1986-1990	2006
T. Terada M. Mizobata S. Kawakami Y. Yabe F. Yamashita M. Hashida	Basic fibroblast growth factor-binding peptide as a novel targeting ligand of drug carrier to tumor cells	Journal of Drug Targeting	14(8)	536-545	2006
Y. Higuchi S. Kawakami M. Oka Y. Yabe F. Yamashita M. Hashida	Intravenous administration of mannosylated cationic liposome/NFkappa B decoy complexes effectively prevent LPS-induced cytokine production in a murine liver failure model	FEBS Letters	580(15)	3706-3714	2006
T. Okuda S. Kawakami T. Maeie T. Niidome F. Yamashita M. Hashida	Biodistribution characteristics of amino acid dendrimers and their PEGylated derivatives after intravenous administration	Journal of Controlled Release	114(1)	69-77	2006
Y. Hattori S. Kawakami K. Nakamura F. Yamashita M. Hashida	Efficient gene transfer into macrophages and dendritic cells by in vivo gene delivery with mannosylated lipoplex via the intraperitoneal route	Journal of Pharmacology and Experimental Therapeutics	318(2)	828-834	2006
Y. Higuchi S. Kawakami S. Fumoto F. Yamashita M. Hashida	Effect of the particle size of galactosylated lipoplex on hepatocyte-selective gene transfection after intraportal administration	Biological and Pharmaceutical Bulletin	29(7)	1521-1523	2006

W. Yeeprae S. Kawakami F. Yamashita M. Hashida	Effect of mannose density on mannose receptor-mediated cellular uptake of mannosylated O/W emulsions by macrophages	Journal of Controlled Release	114(2)	193-201	2006
S. Kawakami Y. Ito P. Charoensit F. Yamashita M. Hashida	Evaluation of proinflammatory cytokine production induced by linear and branched polyethylenimine/plasmid DNA complexes in mice	Journal of Pharmacology and Experimental Therapeutics	317(3)	1382-1390	2006
T. Terada M. Iwai S. Kawakami F. Yamashita M. Hashida	Novel PEG-matrix metalloproteinase-2 cleavable peptide-lipid conntaining galactosylated liposomes for hepatocellular carcinoma-selective targeting	Journal of Controlled Release	111(3)	333-342	2006
Y. Hattori S. Kawakami Y. Lu K. Nakamura F. Yamashita M. Hashida	Enhanced DNA vaccine potency by mannosylated lipoplex after intraperitoneal administration	Journal of Gene Medicine	8(7)	824-834	2006
Y. Higuchi S. Kawakami M. Oka F. Yamashita M. Hashida	Suppression of TNFa production in LPS induced liver failure mice after intravenous injection of cationic liposome/NFκB decoy complex	Pharmazie	61(2)	144-147	2006

Journal of Controlled Release

Full length paper

Optimization of tumor-selective targeting by basic fibroblast growth factor-binding peptide grafted PEGylated liposomes

Takeshi Terada, Miki Mizobata, Shigeru Kawakami, Fumiyoshi Yamashita, and Mitsuru Hashida *

Department of Drug Delivery Research, Graduate School of Pharmaceutical Sciences, Kyoto University, Kyoto 606-8501, Japan.
*Correspondence: M. Hashida, Department of Drug Delivery Research, Graduate School of Pharmaceutical Sciences, Kyoto University, Kyoto 606-8501, Japan. Tel: 81 75 753 4525. Fax: 81 75 753 4575. E-mail: hashidam@pharm.kyoto-u.ac.jp

Abstract

We have previously shown that the peptide, KRTGQYKLC (bFGF), is recognized by fibroblast growth factor (FGF) receptor (FGFR) via binding to basic FGF (bFGF), and is capable of being used for drug delivery to tumors highly expressing FGFR and bFGF. However, although the binding and uptake of the liposomes (bFGFp-liposomes) modified by the peptide increased in the presence of bFGF, the modification induced non-specific uptake. To overcome this problem, here, we prepared bFGFp-liposomes including mPEG-DSPE. The 5 and 10% $mPEG_{5000}$/ and 10% $mPEG_{3000}$/bFGFp-liposomes reduced most of the interaction with erythrocytes and the uptake by macrophages, suggesting the sustained blood circulation of bFGFp grafted PEGylated liposomes. Furthermore, 10% $mPEG_{3000}$/bFGFp-liposomes produced a significant increase in uptake in NIH3T3, A549, and B16BL6 cells with the expression of FGFR following pre-incubation with bFGF, but no increase in CHO-K1 cells lacking FGFR expression. Taken together, these results lead us to believe that bFGFp grafted PEGylated liposomes possess the functions of both PEGylated stealth liposomes and the tumor-targeting liposomes. This strategy could be applied to the development of novel tumor-selective drug delivery systems.

Keywords: Drug delivery system; Liposomes; Targeting; bFGFp-liposomes, Cancer

1. Introduction

Tumor cells, such as melanoma, breast cancer, and prostate cancer, are reported to exhibit overexpression of basic fibroblast growth factor (bFGF) and FGF receptors (FGFR) (1-3). Furthermore, such tumors have high concentrations of bFGF (4), a multi-functional protein, which has mitogenic, chemotactic, and angiogenic activities and plays an autocrine role in tumor angiogenesis and progression (5-9).

It has been reported that residues 117-126 of bFGF might interact with bFGF itself (10). Recently, we have shown that the peptide KRTGQYKLC (bFGFp) containing cysteine at the carboxyl terminal of residues 119-126 of bFGF is able to bind to bFGF and is recognized by FGFR via this binding (11). The binding of bFGFp to bFGF was also higher than that to albumin which is the major serum protein, and the dissociation constant was very low. Based on these findings, we have demonstrated that bFGFp grafted liposomes (bFGFp-liposomes) are specifically taken up by tumor cells highly expressing FGFR via binding to bFGF, suggesting that it could be used as a novel drug delivery carrier to target tumors. However, it was also shown that the non-specific binding of bFGFp-liposomes by bFGFp is high. Therefore, further optimization is needed to reduce the non-specific binding for the *in vivo* use of bFGFp-liposomes for tumor-specific targeting.

It has been reported that polyethyleneglycol (PEG)-grafted liposomes are not highly recognized by the reticulo-endothelial system (RES) and they remain longer in the blood circulation than conventional liposomes (12-15). Accordingly, in the design of bFGFp-liposomes, one approach is to conjugate bFGFp to the liposomal PEG terminals. This strategy has been reported to be an effective targeting approach to reduce non-specific binding (16). However, Savva et al. showed that PEG-grafted liposomes bearing genetically modified recombinant tumor necrosis factor-α on the PEG terminals exhibited rapid plasma elimination and high accumulation in liver and spleen (17). Furthermore, they suggested that not all biological molecules are suitable as targeting ligands when exposed to the grafted PEG extremities of liposomes circulating for long periods. Since bFGFp contains many basic amino residues, the bFGFp-liposomes possess a positive charge on the liposomal surface even if pFGFp is conjugated to the liposomal PEG terminals. The positive charge may induce rapid uptake by RES and non-specific binding with unexpected cells, such as erythrocytes, after intravenous administration.

In the present study, to overcome this problem, we prepared bFGFp-liposomes containing mPEG-DSPE (bFGFp grafted PEGylated liposomes). This mPEG is expected to limit the interactions with RES and other non-target cells. Therefore, we evaluated the inhibitory effects on the uptake by macrophages, used as model cells of the RES, and the interaction with erythrocytes *in vitro*. Furthermore, the binding of bFGFp grafted PEGylated liposomes to bFGF can induce the specific uptake by the tumor cells expressing FGFRs due to the protrusion of the binding bFGF from the PEG layer.

2. Materials and Methods

2.1. Materials

Recombinant human bFGF was obtained from PeproTech EC. (London, UK). Recombinant human FGFR1α (IIIc)/Fc chimera (FGFR1) was purchased from Techne Co. (Minneapolis, MN, USA). Distearoyl phosphatidylcholine (DSPC) was purchased from Sigma-Aldrich Co. (St. Louis, MO, USA). Cholesterol (Chol) and Clear-Sol I were obtained from Nacalai Tesque Inc. (Kyoto, Japan). [^{3}H] CHE was purchased from NEN Life Science Products Inc. (Boston, MA, USA). The peptide KRTGQYKLC (bFGFp) was custom-made by Toray Research Center Inc. (Tokyo, Japan). $mPEG_{3000}$-DSPE was purchased from Avanti Polar Lipids Inc. (Alabama, AL, USA). $mPEG_{3000}$-DSPE and Maleimide-PEG_{2000}-DSPE was purchased from NOF Co. Inc. (Tokyo, Japan). All other chemicals were reagent grade products obtained commercially.

2.2. Cell lines

NIH3T3 mouse fibroblasts, A549 human lung cancer cells, and B16BL6 mouse melanoma cells were routinely grown in DMEM medium supplement with 10% FBS, 100 IU/mL penicillin, 100 μg/mL streptomycin, and 2 mM L-glutamine (all from Invitrogen Co., Carlsbad, CA, USA) in 5% CO_2, humidified air at 37 ºC. Chinese hamster ovary (CHO)-K1 cells were cultured in Ham's F12 medium supplemented with 10% FBS.

2.3. Synthesis of bFGFp-PEG-DSPE

Synthesis of bFGFp-PEG-DSPE was carried out by the method described previously (11). Briefly, 28 mg bFGFp (26 μmol) was dissolved in 2 mL 0.1 M HEPES buffer (pH 7.0) then 50 mg maleimide-PEG_{2000}-DSPE (17 μmol) and 0.2 mL methanol were added to the bFGFp solution at 4 ºC while stirring. The reaction was continued at 4 °C for 2 days. To remove the unreacted bFGFp, the solution was dialyzed against distilled water using a suitable dialysis membrane (3.5 kDa cut-off), and lyophilized. TLC analysis and ninhydrin assay showed the disappearance of free maleimide-PEG_{2000}-DSPE and the appearance of bFGFp-PEG_{2000}-DSPE, indicating that the reaction had gone to completion. The purity of the synthesized bFGFp-PEG-DSPE was calculated by fluorescamine assay (18) and found to be over 90% on the basis of the bFGFp amino acids. Furthermore, 10 mM L-cysteine solution and the product were mixed at room temperature for 1 h to consume any free maleimide-PEG_{2000}-DSPE, followed by dialysis and lyophilization.

2.4. Preparation of liposomes

Liposomes were prepared by our previously reported method (19-21). Each lipid mixture (DSPC, Chol, $mPEG_{3000}$-DSPE, and $mPEG_{5000}$-DSPE) was dissolved in chloroform and evaporated to dryness. bFGFp-PEG-DSPE was solved in a mixed organic solvent (chloroform:methanol = 1:1) beforehand. [^{3}H] CHE or PE-fluorescein (1 mol %) was added to the liposomes for the uptake study and confocal microscopy, respectively. The dried lipid films were hydrated in PBS, sonicated at 65 °C for 3 min, and then extruded through 0.2 μm pore size polycarbonate filters. Mean particle diameters were determined by laser light scattering using a Zetasizer Nano ZS instrument (Malvern Instruments, Malvern, UK). All liposomes were similar in size (an average diameter of approximately 100 nm) as shown in Table 1.

2.5. Quartz crystal microbalance (QCM) biosensor system

Binding analysis between bFGF and bFGFp-liposomes was performed with a 27 MHz QCM instrument (AffinixQ, Initium Inc, Tokyo, Japan). bFGF was immobilized on a ceramic sensor chip using an amine coupling reaction. A drop of 5 mM DTDP was applied to a sensor chip to immobilize the DTDP directly on the gold electrode surface of the chip by an Au–thiol interaction. After 24 h, the sensor chip was then activated by adding a coupling solution including 50 mg/mL EDC and 50 mg/mL NHS. Immobilization of bFGF onto the QCM was achieved by coating the surface with 50 μg/mL bFGF solutions for 2 h at room temperature, followed by rinsing with water. To block the activated surface and nonspecific binding sites, the surface was exposed to 50 mM Tris buffer (pH 8.0) and the purchased blocking solution (Initium Inc., Tokyo, Japan) for 30 min and then washed with water. After immersing the prepared sensor chip in 8 mL 10 mM HEPES buffer (pH 7.4) containing 150 mM NaCl, with gentle stirring at 37 °C, each sample was added to the buffer and the interaction was investigated by monitoring the alterations in frequency (ΔF) resulting from changes in mass at the electrode surface.

Binding analysis between erythrocytes and each mPEG/bFGFp-liposome preparation was performed with a 27 MHz QCM instrument. Fresh blood from male ICR mice was collected in a heparinized syringe. The mice were obtained from Shizuoka Agricultural Co-operative Association for Laboratory Animals (Shizuoka, Japan). Erythrocytes were washed three times on ice in order to remove serum proteins and resuspended in 10 mM HEPES buffer (pH 7.4) containing 150 mM NaCl. Erythrocytes were immobilized on a ceramic sensor chip by an amine coupling reaction. Briefly, 10% erythrocyte suspension (erythrocyte volume/erythrocyte suspension volume %) was added to the activated surface of the sensor chip by the method described above. After 1 h at 4 °C, the surface was rinsed with PBS. To block the activated surface and nonspecific binding sites, the surface was exposed to 50 mM Tris buffer (pH 8.0) containing 150 mM NaCl and the purchased blocking solution (initium Inc., Tokyo, Japan) for 30 min at 4 °C and then washed with PBS. After immersing the prepared sensor chip in 8 mL 10 mM HEPES buffer (pH 7.4) containing 150 mM NaCl, with gentle stirring at 37 °C, each liposome preparation was added to the buffer in the following order: 10 and 5% $mPEG_{5000}$/bFGFp-liposomes, 10% $mPEG_{3000}$-bFGFp-liposomes, and bFGFp-liposomes. The interaction was investigated by monitoring alterations in frequency (ΔF) resulting from changes in mass at the electrode surface.

2.6. Surface plasmon resonance (SPR) spectroscopy assay

SPR measurement was performed using a BIAcore X instrument (BIAcore, Uppsala, Sweden) by our previously reported method (11, 22). FGFR1 was immobilized on the surface of a CM5 sensor chip using the standard amine coupling procedure of the manufacturer. Briefly, the surface of the chip consisting of flow cells 1 and 2 was activated by exposing them to a mixture of 0.05 M *N*-hydroxysuccinimide (NHS) and 0.2 M *N*-ethyl-*N'*-dimethylaminopropyl carbodiimide (EDC) for 7 min. Flow cell 1 was immobilized with FGFR1 in acetate buffer (pH 4.0). The amount of the immobilization was approximately 5000 resonance units (RU). Flow cell 2 was immobilized with the same amount as flow cell 1 by BSA to be used as a blank sensorgram for subtraction of the bulk refractive index background. Finally, the unreacted sites of both immobilized flow cells were blocked with 0.1 M ethanolamine (pH 8.5). All reagents were injected at a flow rate of 5 μL/min.

In the binding measurements, each sample was adjusted to an appropriate concentration by using a buffer (10 mM HEPES, 150 mM NaCl, pH 7.4). Each sample solution was allowed to flow at 20 μL/min for 3 min at 25 °C and dissociated for 3 min. The regeneration of the sensor chip was carried out by injection of 50 mM HCl.

2.7. Cellular uptake study in macrophages

A cellular uptake study in macrophages was performed using our previously reported method (23). Briefly, five-week-old male ICR mice were obtained from Shizuoka Agricultural Co-operative Association for Laboratory Animals (Shizuoka, Japan). Resident macrophages were collected from the peritoneal cavity of unstimulated mice with serum free RPMI 1640 medium. Washed cells were suspended in RPMI 1640 medium supplemented with serum and plated on 12-well culture plates at a density of 1×10^6 cells / well. After incubation for 2 h at 37 °C in 5% CO_2 - 95% air, adherent macrophages were washed three times with RPMI 1640 medium to remove non-adherent cells and then cultured under the same conditions. After 48 h incubation, the cells were washed 3-times and incubated with HBSS containing 100 μM (total lipids) of each [^{3}H] liposome form at 37 °C for 2 h. The radioactivity was measured as described above.

2.8. Cellular association experiments

A cellular association study was performed using our previously reported method (11, 23). Briefly, NIH3T3, A549 and CHO-K1 cells were plated on 12-well culture plates at a density of 1×10^5 cells/well. After 24 h incubation, cells were washed three times with Hanks' balanced salt solution (HBSS) and incubated with 100 μM (total lipids) of each [^{3}H] liposome form, with or without

pretreatment of 1 μg/mL bFGF, for the indicated time in HBSS at 37 °C. After 5 h, the solution was removed and cells were washed with ice-cold HBSS. Cells were then solubilized with 0.3 N NaOH with 0.1 % Triton-X-100 and the radioactivity in the cell lysate was measured using a well-type NaI-scintillation counter (ARC-500, Aloka, Tokyo, Japan). The amount of cellular protein in each cell lysate was estimated using a protein quantification kit (Dojindo Laboratory).

2.9. Confocal microscopic study

The confocal microscopic study was performed using a standard method (24, 25). Briefly, NIH3T3, A549, and B16BL6 cells were seeded on glass coverslips in 12-well plates at a density of 1×10^5 cells/well. After complete adhesion, the cells were washed 3times with HBSS and incubated at 4 or 37 °C for 5 h with the fluorescent 10% $mPEG_{3000}$/bFGFp-liposomes, with or without the pretreatment of 1 μg/mL bFGF, for 24 h in HBSS. After incubation, the liposome solution was removed, and the cells were washed 3 times with HBSS, followed by fixing with 4% parafolmaldehyde in PBS, and incubating at room temperature for more than 20 min. After washing twice with PBS, the cells were mounted in glycerol:PBS (1:1) containing 2.5% 1,4-diazobicyclo (2,2,2) octane. Images were obtained by confocal laser scanning microscopy (MRC-1024, Bio-Rad, Hercules, CA, USA).

2.10. Statistical analysis

Statistical analysis was performed using Student's paired *t*-test for two groups. Multiple comparisons with the control group were performed by ANOVA with Dunnett's multiple-comparison test. $P < 0.05$ was considered to be indicative of statistical significance.

3. Results

3.1. Interaction analysis of bFGFp-liposomes with bFGF

The interaction of bFGFp-liposomes with bFGF was investigated using the QCM biosensor system (Fig. 1). The 27-MHz QCM biosensor system used in this study has a sensitivity of 0.6 ng cm^{-2} of mass change per 1 Hz of frequency decrease (26). bFGF was immobilized on a sensor chip coated with DTDP by amine coupling. Fig. 1 shows the typical frequency changes for the bFGF-immobilized QCM sensor chip, responding to additions of mPEG-liposomes or bFGFp-liposomes in solution. The addition of mPEG-liposomes produced no change in the frequency (mass). On the other hand, in the case of bFGFp-liposomes, the frequency decreased (mass increased), and the decrease was inhibited by the presence of excess bFGFp. Therefore, the frequency decrease indicated by the addition of bFGFp-liposomes is consistent with the mass increase due to the binding of bFGFp-liposomes to bFGF via the bFGFp present in the QCM biosensor system.

3.2. The binding of bFGFp-liposomes to FGFR1 via bFGF

Recently, we used SPR spectroscopy to show that BSA modified by bFGFp (bFGFp-BSA) interacts with FGFR1 via binding to bFGF (11). Here, we confirmed the interaction of bFGFp-liposomes with FGFR1 via binding to bFGF using the same method as in the previous report (11) (Fig. 2). FGFR1 was immobilized on the surface of a CM5 sensor chip by amine coupling. Non-specific binding of an analyte and any change in bulk refractive index were eliminated by immobilizing BSA as a control. Although bFGF showed a significantly high response signal (Fig. 2), no response signal was observed with bFGFp-liposomes. In addition, the response signal of bFGFp-liposomes pre-incubated with bFGF was much higher than that of bFGF itself, suggesting that bFGFp-liposomes pre-incubated with bFGF are capable of binding to FGFR1 via bFGF. These results were in good agreement with our previous report using bFGFp-BSA (11).

3.3. The effect of mPEG-DSPE on the uptake of bFGFp-liposomes by macrophages

Our previous study showed that bFGFp-liposomes exhibit a high degree of unspecific uptake in cells (11). As shown in Fig. 3, we also found a high uptake by macrophages used as model cells of mononuclear phagocytes in the RES. The high uptake by macrophages would lead to a reduced targeting efficiency to the tumor cells because of the high trapping by RES after intravenous administration. Therefore, we prepared mPEG/bFGFp-liposomes, without or with 1, 2.5, 5, and 10% of $mPEG_{5000}$-DSPE and $mPEG_{3000}$-DSPE, to reduce the non-specific binding and/or uptake. The cellular association in macrophages decreased with an increase in the amount of mPEG-DSPE. In particular, mPEG/bFGFp-liposomes containing 5 or 10% $mPEG_{5000}$-DSPE (Fig. 3 (A)) and 10% $mPEG_{3000}$-DSPE (Fig. 3 (B)) showed a significantly reduced uptake, suggesting prolonged circulation in the body after intravenous administration.

3.4. The effect of mPEG-DSPE on the interaction of mPEG/bFGFp-liposomes with erythrocytes

Furthermore, the effect of mPEG-DSPE on the interaction of mPEG-bFGFp-liposomes with erythrocytes was evaluated using a QCM biosensor system. Fig. 4 shows the typical frequency changes for the isolated erythrocyte-immobilized QCM sensor chip, responding to additions of each form of liposomes in the following order: 10 and 5% $mPEG_{5000}$/bFGFp-liposomes, 10% $mPEG_{3000}$/bFGFp-liposomes, and bFGFp-liposomes. The three kinds of mPEG/bFGFp-liposomes indicating the controlled uptake in macrophages exhibited no change in frequency (mass) in the QCM biosensor system, suggesting no interaction with erythrocytes. On the other hand, the frequency decreased (mass increased) following the addition of bFGFp-liposomes. The three

mPEG/bFGFp-liposomes are capable of controlling the interaction with erythrocytes via the bFGFp present on the surface of the liposomes.

3.5. The effect of bFGF on the uptake of mPEG/bFGFp-liposomes by various cells

The cellular uptake via bFGF of the three mPEG/bFGFp-liposomes was examined (Fig. 5). NIH3T3 and A549 cells express FGFR, and CHO-K1 cells are known to lack these receptors (27). In these cells with or without FGFRs, the uptake of mPEG/bFGFp-liposomes was almost the same as that in macrophages, suggesting that the each incorporation of 5 or 10%mPEG5000-DSPE and 10% mPEG3000-DSPE is enough to inhibit the non-specific cellular uptake of bFGFp-liposomes. Furthermore, pre-incubation of $mPEG_{3000}$/bFGFp-liposomes with bFGF produced a significant increase in the uptake in NIH3T3 and A549 cells. However, CHO-K1 cells exhibited no such increase while the two PEG_{5000}/bFGFp-liposomes exhibited no uptake in NIH3T3 and A549 cells, even if pre-incubated with bFGF.

3.6. The binding or internalization of $mPEG_{3000}$/bFGFp-liposomes to cells

To further demonstrate the binding of the labeled $mPEG_{3000}$/bFGFp-liposomes with PE-fluorescein via bFGF to cells using confocal microscopy, the liposomes were incubated with NIH3T3 cells at 4 °C. Fluorescent signals of the liposomes pre-incubated with bFGF were observed on the surface of the cells, and these were much stronger than those of liposomes without bFGF (Fig. 6). In addition, the cellular internalization of the liposomes by confocal microscopy was examined in NIH3T3, A549, and B16BL6 cells, all of which are known to express FGFR (Fig. 7). In all the cells used, the images showed that the liposomes pre-incubated with bFGF were internalized, and the fluorescent signal was stronger than that of the liposomes without bFGF. These results were in good agreement with our previous study of cellular internalization using bFGFp-BSA.

3.7. The effect of the pre-incubation time of $mPEG_{3000}$/bFGFp-liposomes with bFGF on the uptake in NIH3T3 cells

$mPEG_{3000}$/bFGFp-liposomes were incubated with bFGF for 1 and 24 h, and the uptakes in NIH3T3 cells were compared with those of liposomes without bFGF (Fig. 8). Although the incubation for 1 h significantly increased the uptake, incubation of $mPEG_{3000}$/bFGFp-liposomes for 24 h produced a higher increase in uptake. In spite of high association of bFGFp with bFGF, it took long time to equilibrate the interaction of mPEG3000/bFGFp-liposomes with bFGF. This suggests that the incorporation of mPEG-DSPE in bFGFp-liposomes hinders the interaction of bFGFp with bFGF, and the successful targeting of the tumor takes some time.

4. Discussion

PEGylation provides drug carriers with steric stabilization, subsequently leading to reduce uptake by the RES and prolonged circulation in the body (15, 28, 29). Pharmacokinetic analysis and therapeutic studies with tumor-bearing mice have shown that PEG-liposomes have considerable potential as drug carriers for tumor therapy. These liposomes can exploit the "enhanced permeability and retention (EPR)" effect (30-32) for preferential extravasation from tumor vessels, which results in increased liposome accumulation in tumor tissues (33, 34). However, to produce more effective targeting of tumor cells, requires the development of novel liposomes exhibiting both a long circulation by PEGylation and the active targeting by the ligand.

In a previous report, we showed that the peptide KRTGQYKLC (bFGFp) can interact with FGFR1 via binding to bFGF, and is useful as the targeting ligand for tumor cells (11). The binding characteristics allow the development of novel PEG-liposomes for tumor therapy. First of all, we confirmed the binding of bFGFp-liposomes to bFGF and FGFR1 by using a QCM biosensor system and SPR spectroscopy, which has been widely used as an instrument to study a variety of biomolecular interactions, including liposome-protein (35, 36), DNA-protein (26) and protein-protein (37, 38). All liposomes were prepared with an average diameter of 100-200 nm (Table 1), which has been reported to result in a prolonged circulation time and high tumor accumulation (39, 40). bFGFp-liposomes interacted with bFGF via bFGFp (Fig. 1) and with FGFR1 via binding to bFGF (Fig. 2). These findings agree with our previous report using bFGFp-BSA (11).

To achieve prolonged blood circulation of bFGFp-liposomes in the body, we prepared mPEG/bFGFp-liposomes by adding mPEG-DSPE to bFGFp-liposomes. The steric hindrance of the added mPEG on the surface of bFGFp-liposomes results in a reduction in the non-specific binding caused by the bFGFp present. In this study, we selected two kinds of mPEG-DSPE containing PEG with an MW of 5000 or 3000. Since the MW of the bFGFp-PEG of the synthesized bFGFp-PEG-DSPE is approximately 3000, it appears that the two mPEG-DSPEs have a sufficient PEG to cover the bFGFp present. The high uptake by macrophages and strong interaction with erythrocytes in bFGFp-liposomes, which leads to early elimination from the blood and a low targeting efficiency, were significantly reduced by the addition of 5 and 10% $mPEG_{5000}$/bFGFp- and 10% $mPEG_{3000}$/bFGFp-liposomes (Figs. 3 and 4). These results lead us to believe that these bFGFp grafted PEGylated liposomes would exhibit a prolonged circulation in the body.

In the bFGFp grafted PEGylated liposomes, the targeting to tumor cells via binding to bFGF indicates the success of novel PEG-liposomes exhibiting both prolonged blood circulation and active tumor targeting. In practical terms, we showed that the pre-incubated $mPEG_{3000}$/bFGFp-liposomes with bFGF exhibit specific binding to the cells expressing FGFR (Fig. 5). The addition of 10% $mPEG_{3000}$-DSPE to bFGFp grafted liposomes abolished the binding by the bFGFp present on the liposomal surface, and the binding of bFGF to bFGFp could allow the targeting of tumor cells via FGFR by protrusion of the binding bFGF from the PEG layer. Furthermore, the receptor-mediated internalization demonstrated by confocal microscopy (Fig. 7) would allow the 10% mPEG3000/bFGFp-liposomes to avoid the action of multidrug resistant (MDR) transporters like P-glycoprotein and enhance the pharmacological effects of the antitumor drug as reported recently (41). We also found that pre-incubation with 10% $mPEG_{3000}$/bFGFp-liposomes enhances the binding on the surface of NIH3T3 cells as shown by an *in vitro* study at 4 °C (Fig. 6),

suggesting that the targeting potential obtained by pre-incubation is not due to the physiological effects of bFGF itself. The difference in uptake between pre-incubation with 10% $mPEG_{3000}$-bFGFp-liposomes for 1 and 24 h also suggests that the targeting is not due to physiological effects (Fig. 8). Furthermore, this result leads us to surmise that targeting via binding to bFGF would take a comparatively long time. Some tumor cells are reported to exhibit overexpression of bFGF and FGFRs (1-3), and such tissues contain high concentrations of bFGF (4). Taking these findings into consideration, liposomes with a prolonged blood circulation may accumulate in tumor tissues containing high concentrations of bFGF by the EPR effect, and subsequently lead to active targeting via binding to bFGF.

$mPEG_{5000}$/bFGFp-liposomes exhibited no targeting effect on cells even if pre-incubated with bFGF. One possible reason for this is that the long PEG-chains could completely inhibit the interaction with bFGF, or else the bFGFp present could bind to bFGF, and the interaction of the bound bFGF with FGFR was blocked by the long PEG-chains on the liposomal surface. This finding agrees with a previous report showing that the immuno-specific antibody-antigen binding by immunoliposomes conjugated with a monoclonal IgG antibody could be reduced by the addition of PEG with an MW of 2000 (42). In the case of complicated binding, such as antibody-antigen and bFGF-FGFR, the addition of short PEG-chains could suppress the targeting effects of ligand-modified liposomes due to steric hindrance.

In the targeting system using ligands such as peptides, species differences area problem as far as successful clinical application is concerned. It has been reported that the homology between murine and human FGF-2 is high (95% homologous) (43). Moreover, the peptide KRTGQYKL used in the present investigation is completely homologous with both murine and human FGF-2. Therefore, further investigation of this strategy will provide us with information about the potential application to tumor therapy in humans.

In conclusion, we have succeeded in the development of novel PEG-liposomes for tumor targeting. mPEG/bFGFp-liposomes were prepared as novel PEG-liposomes by adding mPEG-DSPE to bFGFp-liposomes capable of targeting tumor cell expressing FGFR via binding to bFGF. The addition of 5 and 10% $mPEG_{5000}$-DSPE and 10% $mPEG_{3000}$-DSPE reduced the uptake by macrophages and interaction with erythrocytes. Furthermore, 10% $mPEG_{3000}$/bFGFp-liposomes exhibited specific targeting of tumor cells via binding to bFGF. Further investigations involving *in vivo* studies, including the interaction with serum proteins and the targeting efficiency of the local bFGF concentrations in tumor tissue, are needed. However, our results suggest that the bFGFp grafted PEGylated liposomes exhibit both prolonged blood circulation by limiting the transfer to normal tissues and active targeting to cells in the tumor tissues. This strategy could be applied to the development of novel tumor-selective drug delivery systems.

Acknowledgments

This work was supported in part by Grant-in-Aids for Scientific Research from the Ministry of Education, Culture, Sports, Science, and Technology of Japan, by Health and Labour Sciences Research Grants for Research on Advanced Medical Technology from the Ministry of Health, Labour and Welfare of Japan, and by the 21st Century COE Program "Knowledge Information Infrastructure for Genome Science".

References

[1] F. Penault-Llorca, F. Bertucci, J. Adelaide, P. Parc, F. Coulier, J. Jacquemier, D. Birnbaum, O. deLapeyriere, Expression of FGF and FGF receptor genes in human breast cancer, Int. J. Cancer 61 (1995) 170-176.

[2] T. Danielsen, E.K. Rofstad, VEGF, bFGF and EGF in the angiogenesis of human melanoma xenografts, Int. J. Cancer 76 (1998) 836-841.

[3] B. Kwabi-Addo, M. Ozen, M. Ittmann, The role of fibroblast growth factors and their receptors in prostate cancer, Endocr. Relat. Cancer 11 (2004) 709-724.

[4] D. Giri, F. Ropiquet, M. Ittmann, Alterations in expression of basic fibroblast growth factor (FGF) 2 and its receptor FGFR-1 in human prostate cancer, Clin. Cancer Res. 5 (1999) 1063-1071.

[5] R. Halaban, S. Ghosh, A. Baird, bFGF is the putative natural growth factor for human melanocytes, In Vitro Cell. Dev. Biol. 23 (1987) 47-52.

[6] R. Halaban, B.S. Kwon, S. Ghosh, P. Delli Bovi, A. Baird, bFGF as an autocrine growth factor for human melanomas, Oncogene Res. 3 (1988) 177-186.

[7] D.A. Lappi, Tumor targeting through fibroblast growth factor receptors, Semin. Cancer Biol. 6 (1995) 279-288.

[8] A. Compagni, P. Wilgenbus, M.A. Impagnatiello, M. Cotten, G. Christofori, Fibroblast growth factors are required for efficient tumor angiogenesis, Cancer Res, 60 (2000) 7163-7169.

[9] J.K. Dow, R.W. deVere White, Fibroblast growth factor 2: its structure and property, paracrine function, tumor angiogenesis, and prostate-related mitogenic and oncogenic functions, Urology 55 (2000) 800-806.

[10] L. Kinsella, H.L. Chen, J.A. Smith, P.S. Rudland, D.G. Fernig, Interactions of putative heparin-binding domains of basic fibroblast growth factor and its receptor, FGFR-1, with heparin using synthetic peptides, Glycoconj. J. 15 (1988) 419-422.

[11] T. Terada, M. Mizobata, S. Kawakami, Y. Yabe, F. Yamashita, M. Hashida, Basic fibroblast growth factor-binding peptide as a novel targeting ligand of drug carrier to tumor cells, J. Drug Target. 14 (2006) 536-545.

[12] T.M. Allen, G.A. Austin, A. Chonn, L. Lin, K.C. Lee, Uptake of liposomes by cultured mouse bone marrow macrophages: influence of liposome composition and size, Biochim. Biophys. Acta 1061 (1991) 56-64.

[13] D.D. Lasic, F.J. Martin, A. Gabizon, S.K. Huang, D. Papahadjopoulos, Sterically stabilized liposomes: a hypothesis on the molecular origin of the extended circulation times, Biochim. Biophys. Acta 1070 (1991) 187-192.

[14] D. Needham, T.J. McIntosh, D.D. Lasic, Repulsive interactions and mechanical stability of polymer-grafted lipid membranes, Biochim. Biophys. Acta 1108 (1992) 40-48.

[15] K. Maruyama, PEG-immunoliposome, Biosci. Rep. 22 (2002) 251-266.

[16] H. Harashima, T. Ishida, H. Kamiya, H. Kiwada, Pharmacokinetics of targeting with liposomes, Crit. Rev. Ther. Drug Carrier Syst. 19 (2002) 235-275.

[17] M. Savva, E. Duda, L. Huang, A genetically modified recombinant tumor necrosis factor-alpha conjugated to the distal terminals of liposomal surface grafted polyethyleneglycol chains, Int. J. Pharm. 184 (1999) 45-51.

[18] P. Bohlen, S. Stein, W. Dairman, S. Udenfriend, Fluorometric assay of proteins in the nanogram range, Arch. Biochem. Biophys.

155 (1973) 213-220.
[19] S. Kawakami, J. Wong, A. Sato, Y. Hattori, F. Yamashita, M. Hashida, Biodistribution characteristics of mannosylated, fucosylated, and galactosylated liposomes in mice, Biochim. Biophys. Acta 1524 (2000) 258-265.
[20] S. Kawakami, C. Munakata, S. Fumoto, F. Yamashita, M. Hashida, Novel galactosylated liposomes for hepatocyte-selective targeting of lipophilic drugs, J. Pharm. Sci. 90 (2001) 105-113.
[21] C. Managit, S. Kawakami, F. Yamashita, M. Hashida, Effect of galactose density on asialoglycoprotein receptor-mediated uptake of galactosylated liposomes, J. Pharm. Sci. 94 (2005) 2266-2275.
[22] T. Terada, M. Nishikawa, F. Ymashita, M. Hashida, Analysis of the molecular interaction of glycosylated proteins with rabbit liver asialoglycoprotein receptors using surface plasmon resonance spectroscopy, J. Pharm. Biomed. Anal. 41 (2006) 966-972.
[23] T. Terada, M. Iwai, S. Kawakami, F. Yamashita, M. Hashida, Novel PEG-matrix metalloproteinase-2 cleavable peptide-lipid containing galactosylated liposomes for hepatocellular carcinoma-selective targeting, J. Control. Release 111 (2006) 333-342.
[24] N. Skalko, R. Peschka, U. Altenschmidt, A. Lung, R. Schubert, pH-sensitive liposomes for receptor-mediated delivery to chicken hepatoma (LMH) cells, FEBS Lett. 434 (1998) 351-356.
[25] P. Opanasopit, Y. Higuchi, S. Kawakami, F. Yamashita, M. Nishikawa, M. Hashida, Involvement of serum mannan binding proteins and mannose receptors in uptake of mannosylated liposomes by macrophages, Biochim. Biophys. Acta 1511 (2001) 134-145.
[26] H. Matsuno, K. Niikura, Y. Okahata, Direct monitoring kinetic studies of DNA polymerase reactions on a DNA-immobilized quartz-crystal microbalance, Chemistry 7 (2001) 3305-3312.
[27] M. Rusnati, C. Urbinati, E. Tanghetti, P. Dell'Era, H. Lortat-Jacob, M. Presta, Cell membrane GM1 ganglioside is a functional coreceptor for fibroblast growth factor 2, Proc. Natl. Acad. Sci. U.S.A. 99 (2002) 4367-4372.
[28] M. Harada-Shiba, K. Yamauchi, A. Harada, I. Takamisawa, K. Shimokado, K. Kataoka, Polyion complex micelles as vectors in gene therapy--pharmacokinetics and in vivo gene transfer, Gene Ther. 9 (2002) 407-414.
[29] N. Nishiyama, S. Okazaki, H. Cabral, M. Miyamoto, Y. Kato, Y. Sugiyama, K. Nishio, Y. Matsumura, K. Kataoka, Novel cisplatin-incorporated polymeric micelles can eradicate solid tumors in mice, Cancer Res. 63 (2003) 8977-8983.
[30] K. Greish, J. Fang, T. Inutsuka, A. Nagamitsu, H. Maeda, Macromolecular therapeutics: advantages and prospects with special emphasis on solid tumour targeting, Clin. Pharmacokinet. 42 (2003) 1089-1105.
[31] T. Nakanishi, S. Fukushima, K. Okamoto, M. Suzuki, Y. Matsumura, M. Yokoyama, T. Okano, Y. Sakurai, K. Kataoka, Development of the polymer micelle carrier system for doxorubicin, J. Control. Release 74 (2001) 295-302.
[32] H. Maeda, J. Wu, T. Sawa, Y. Matsumura, K. Hori, Tumor vascular permeability and the EPR effect in macromolecular therapeutics: a review, J. Control. Release 65 (2000) 271-284.
[33] J.W. Park, Liposome-based drug delivery in breast cancer treatment, Breast Cancer Res. 4 (2002) 95-99.
[34] A. Di Paolo, Liposomal anticancer therapy: pharmacokinetic and clinical aspects, J. Chemother. 4 (2004) 90-93.
[35] K. Yun, E. Kobatake, T. Haruyama, M.L. Laukkanen, K. Keinanen, M. Aizawa, Use of a quartz crystal microbalance to monitor immunoliposome-antigen interaction, Anal. Chem. 70 (1998) 260-264.
[36] T. Terada, M. Nishikawa, F. Yamashita, M. Hashida, Influence of cholesterol composition on the association of serum mannan-binding proteins with mannosylated liposomes, Biol. Pharm. Bull. 29 (2006) 613-618.
[37] S. Lin, C.C. Lu, H.F. Chien, S.M. Hsu, An on-line quantitative immunoassay system based on a quartz crystal microbalance, J. Immunol. Methods 239 (2000) 121-124.
[38] T. Terada, M. Nishikawa, F. Yamashita, M. Hashida, Analysis of the molecular interaction between mannosylated proteins and serum mannan-binding lectins, Int. J. Pharm. 316 (2006) 117-123.
[39] O. Ishida, K. Maruyama, K. Sasaki, M. Iwatsuru, Size-dependent extravasation and interstitial localization of polyethyleneglycol liposomes in solid tumor-bearing mice, Int. J. Pharm. 190 (1999) 49-56.
[40] G.J. Charrois, T.M. Allen, Rate of biodistribution of STEALTH liposomes to tumor and skin: influence of liposome diameter and implications for toxicity and therapeutic activity, Biochim. Biophys. Acta 1609 (2003) 102-108.
[41] P. Sapra, T.M. Allen, Ligand-targeted liposomal anticancer drugs, Prog. Lipid Res. 42 (2003) 439-462.
[42] K. Maruyama, T. Takizawa, T. Yuda, S.J. Kennel, L. Huang, M. Iwatsuru, Targetability of novel immunoliposomes modified with amphipathic poly(ethylene glycol)s conjugated at their distal terminals to monoclonal antibodies, Biochim. Biophys. Acta 1234 (1995) 74-80.
[43] S.M. Plum, J.W. Holaday, A. Ruiz, J.W. Madsen, W.E. Fogler, A.H. Fortier, Administration of a liposomal FGF-2 peptide vaccine leads to abrogation of FGF-2-mediated angiogenesis and tumor development, Vaccine 19 (2000) 1294-1303.

Figure legends

Fig. 1. QCM assay of binding to the immobilized bFGF for mPEG-liposomes and bFGFp (2.5%)-liposomes, with or without 50 μg/mL bFGFp. Two μM (total lipids) liposomes were injected over immobilized bFGF. Each response signal was overlaid and zeroed on the y-axis to the average baseline. The start injection time for each form of liposomes was set to zero on the x-axis.

Fig. 2. SPR sensorgrams of binding with the immobilized FGFR1 for 5 μg/mL bFGF, and 100 μM (total lipids) bFGFp (2.5%)-liposomes, with or without 5 μg/mL bFGF. Each sensorgram was overlaid and zeroed on the y-axis to the average baseline. The start injection time for each form of liposomes was set to zero on the x-axis.

Fig. 3. Effect of the content and length of mPEG-DSPE on the uptake of [^{3}H] mPEG/bFGFp-liposomes (□) by mouse peritoneal macrophages. Peritoneal macrophages were incubated with $mPEG_{5000}$/bFGFp-liposomes (A) and $mPEG_{3000}$/bFGFp-liposomes (B) containing different amounts of mPEG-DSPE at 37 °C for 2 h. The uptake of [^{3}H] bFGFp-liposomes (■) was used as a comparison. Each result represents the mean ± S.D. values (n = 3). Statistical significance was analyzed by Dunnett's test versus bFGFp-liposomes (**, $P < 0.01$; N.S., not significant).

Fig. 4. QCM assay of binding to the immobilized erythrocytes for mPEG/bFGFp-liposomes and bFGFp-liposomes. Two μM liposomes were injected over immobilized erythrocytes in the following order: 10% $mPEG_{5000}$/bFGFp-liposomes (A), 5 % $mPEG_{5000}$/bFGFp-liposomes (B), 10% $mPEG_{3000}$/bFGFp-liposomes (C), and bFGFp-liposomes (D).

Fig. 5. Effect of bFGF on the cellular association of [^{3}H] mPEG/bFGFp-liposomes by different cells. 10% $mPEG_{5000}$/bFGFp-liposomes,

5% $mPEG_{5000}$/bFGFp-liposome, and 10% $mPEG_{3000}$/bFGFp-liposomes were pre-incubated with bFGF at 37 °C for 24 h. NIH3T3 (A), A549 (B), and CHO-k1 (C) cells were incubated with the mPEG/bFGFp-liposomes without (■) or with (□) the pre-incubation of bFGF at 37 °C for 5 h. Each result represents the mean ± S.D. values (n = 3). Statistical significance was analyzed by Student's t-test versus each group without the pre-incubation of bFGF (**, $P < 0.01$; ***, $P < 0.001$; N.S., not significant).

Fig. 6. Conforcal microscopy images of the binding of 10% $mPEG_{3000}$/bFGFp-liposomes by NIH3T3 cells. NIH3T3 cells were incubated with 10% $mPEG_{3000}$/bFGFp-liposomes containing 1% PE-fluorescein, without or with the pre-incubation of bFGF at 4 °C for 5 h.

Fig. 7. Confocal microscopy images of the binding and internalization of 10 % $mPEG_{3000}$/bFGFp-liposomes by various cells. NIH3T3 (A, D), A549 (B, E), and B16BL6 cells (C, F) were incubated with 10 % $mPEG_{3000}$/bFGFp-liposomes containing 1% PE-fluorescein, without (A, B, C) or with (D, E, F) the pre-incubation of bFGF at 37 °C for 5 h.

Fig. 8. Effect of the preincubation time with bFGF on the cellular association of [^{3}H] $mPEG_{3000}$/bFGFp-liposomes by NIH3T3 cells. 10% $mPEG_{3000}$/bFGFp-liposomes pre-incubated with bFGF for the indicated times were used for the uptake study. Each result represents the mean ± S.D. values (n = 3).

Table 1. Lipid composition and mean particle size of liposomes investigated

Lipid composition (molar ratio)	Particle size (nm)[a]
mPEG-liposomes (DSPC/Chol/mPEG-DSPE =60:37.5:2.5)	101 ± 1.71
bFGFp-liposomes (DSPC/Chol/bFGFp-PEG-DSPE =60:37.5:2.5)	100 ± 1.76
1% $mPEG_{3000}$/bFGFp-liposomes (DSPC/Chol/bFGFp-PEG-DSPE/$mPEG_{3000}$-DSPE=60:36.5:2.5:1)	115 ± 1.99
2.5% $mPEG_{3000}$/bFGFp-liposomes (DSPC/Chol/bFGFp-PEG-DSPE/$mPEG_{3000}$-DSPE=60:35:2.5:2.5)	113 ± 7.06
5% $mPEG_{3000}$/bFGFp-liposomes (DSPC/Chol/bFGFp-PEG-DSPE/$mPEG_{3000}$-DSPE=60:32.5:2.5:5)	114 ± 0.651
10 mol% $mPEG_{3000}$/bFGFp-liposomes (DSPC/Chol/bFGFp-PEG-DSPE/mPEG-$DSPE_{3000}$=60:27.5:2.5:10)	101 ± 1.36
1% $mPEG_{5000}$/bFGFp-liposomes (DSPC/Chol/bFGFp-PEG-DSPE/$mPEG_{5000}$-DSPE=60:36.5:2.5:1)	116 ± 0.961
2.5 % $mPEG_{5000}$/bFGFp-liposomes (DSPC/Chol/bFGFp-PEG-DSPE/$mPEG_{5000}$-DSPE=60:35:2.5:2.5)	113 ± 1.21
5% $mPEG_{5000}$/bFGFp-liposomes (DSPC/Chol/bFGFp-PEG-DSPE/$mPEG_{5000}$-DSPE=60:32.5:2.5:5)	106 ± 1.26
10% $mPEG_{5000}$/bFGFp-liposomes (DSPC/Chol/bFGFp-PEG-DSPE/$mPEG_{5000}$-DSPE=60:27.5:2.5:10)	101 ± 5.02

[a] The mean particle sizes of the liposomes were measured using a laser light scattering particle size analyzer. Results are expressed as the mean ± S.D. of three experiments.

Fig. 1

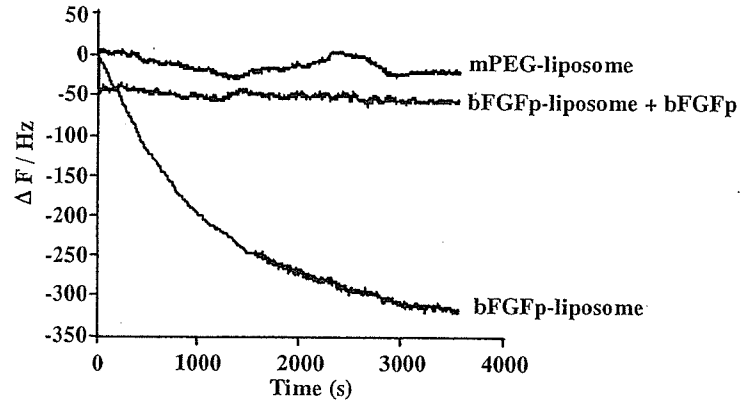

Fig. 2

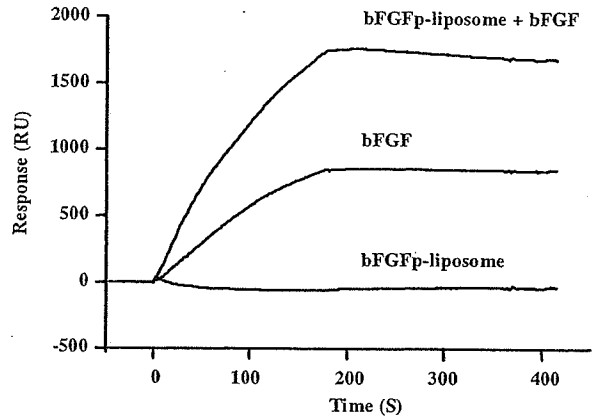

Fig. 3

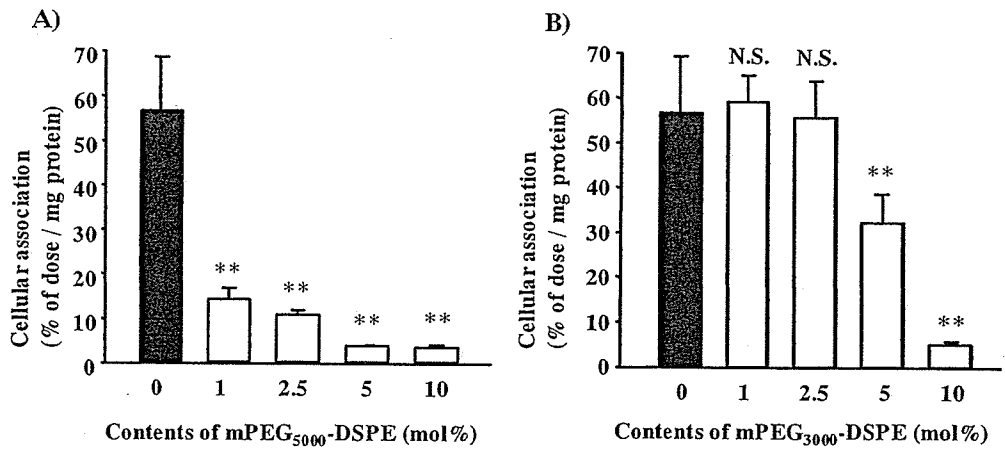

Fig. 4

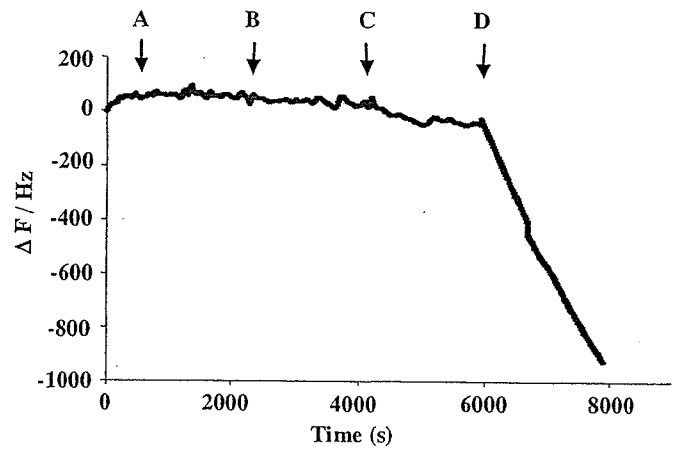

Fig. 5

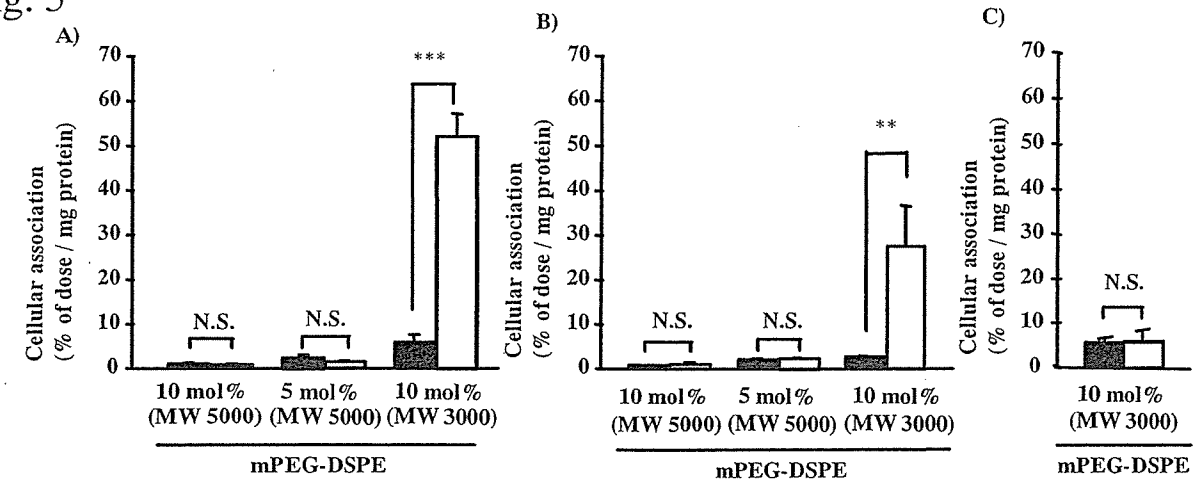

Fig. 6

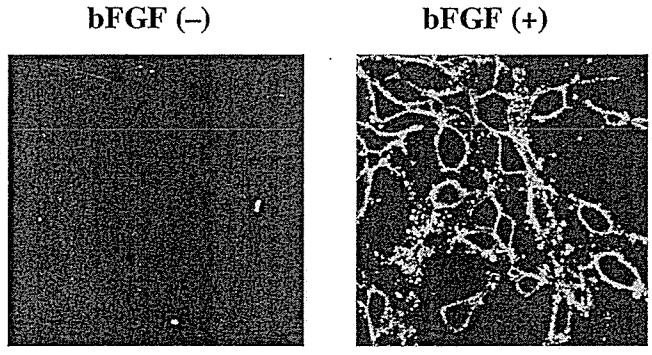

Fig. 7

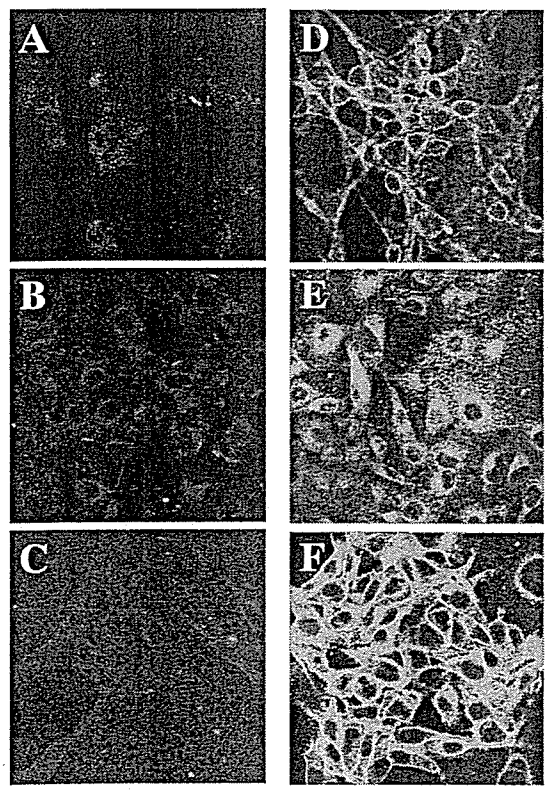

Fig. 8

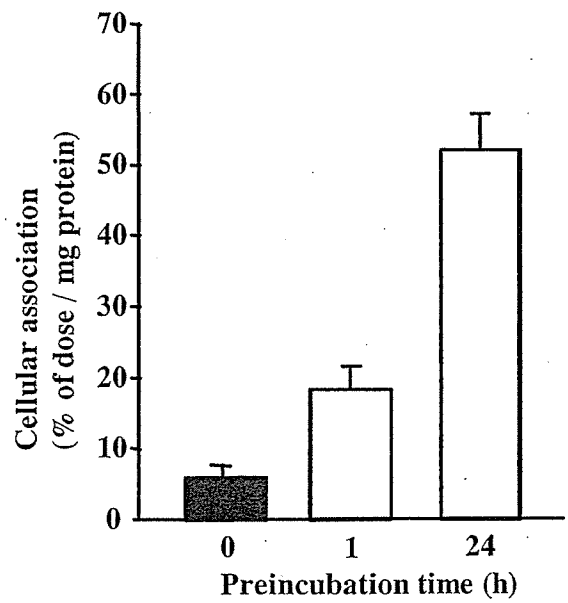

Available online at www.sciencedirect.com
ScienceDirect
Biomaterials 28 (2007) 532–539
Biomaterials
www.elsevier.com/locate/biomaterials

The potential role of fucosylated cationic liposome/NFκB decoy complexes in the treatment of cytokine-related liver disease

Yuriko Higuchi, Shigeru Kawakami, Fumiyoshi Yamashita, Mitsuru Hashida*

Department of Drug Delivery Research, Graduate School of Pharmaceutical Sciences, Kyoto University, Kyoto 606-8501, Japan

Received 15 June 2006; accepted 25 August 2006
Available online 18 September 2006

Abstract

Cytokine production by Kupffer cells, which is regulated by NFκB, causes severe liver injury in endotoxin syndrome. NFκB decoy has been reported to inhibit NFκB-mediated transcription. The purpose of this study is to inhibit LPS-induced cytokine production by Kupffer cell-targeted delivery of NFκB decoy using fucosylated cationic liposomes (Fuc-liposomes). Cholesten-5-yloxy-*N*-{4-[(1-imino-2-L-thiofucosyl-ethyl)-amino] butyl-}formamide (Fuc-C4-Chol) was synthesized to prepare Fuc-liposomes. Tissue accumulation, intrahepatic distribution and serum cytokine concentrations were investigated after intravenous injection of Fuc-liposomes/NFκB decoy complexes. Intravenously injected Fuc-liposome complexes rapidly and highly accumulated in the liver while little naked NFκB decoy accumulated in the liver. An intrahepatic distribution study showed that Fuc-liposome complexes are mainly taken up by non-parenchymal cells. The liver accumulation of Fuc-liposome complexes was inhibited by $GdCl_3$ pretreatment, which selectively inhibited Kupffer cell uptake. This result suggested that Kupffer cells contribute to liver accumulation. TNFα, IFNγ, ALT and AST serum levels in LPS-infected mice were significantly attenuated by treatment with Fuc-liposome complexes compared with naked NFκB decoy. Fuc-liposome complexes also reduced the amount of activated NFκB in the liver nuclei. Fuc-liposomes would be a useful carrier for Kupffer cell-selective delivery of NFκB decoy by intravenous injection.

Keywords: Fucosylated cationic liposome; Gene delivery; Gene therapy; Targeting; NFκB decoy; Kupffer cell

1. Introduction

Several forms of hepatic failure, including endotoxin syndrome, are associated with inflammatory cytokines produced by Kupffer cells [1,2]. Since NFκB regulates inflammatory cytokine production [3,4] the inhibition of NFκB activation in Kupffer cells would offer a new treatment for liver failures. Recently, Wrighton et al. [5] and Foxwell et al. [6] reported that the adenoviral gene transfer of super-repressor IκB effectively suppressed NFκB, however the inflammatory reaction and high immunogenicity of the adenoviral vector itself presented a serious obstacle. On the other hand, it was demonstrated recently that NFκB decoy inhibited the production of cytokines, such as TNFα, IL-1β, IFNγ and IL-12 [7–9]. Therefore, NFκB decoy would be an attractive option for the treatment of cytokine-related liver diseases without any marked immunogenic effects [10].

To establish NFκB decoy therapy, it is necessary to develop a Kupffer cell-targeting carrier for NFκB decoy because of the low uptake of naked NFκB decoy by cells [11]. In general, the receptor-mediated endocytosis system is potentially useful for cell-specific delivery, including carbohydrate receptors expressed on liver cells [12]. As far as gene delivery is concerned, we have shown that mannosylated cationic liposomes can deliver pDNA to NPC [13–15] including Kupffer cells and sinusoidal endothelial cells through the recognition of mannose receptors highly expressed on NPC.

Regarding Kupffer cell-selective delivery, we have demonstrated that fucosylated protein is preferentially taken up by Kupffer cells [16] through fucose receptor recognition, which is uniquely exhibited by Kupffer cells [17]. Taking this into consideration, we have synthesized a

*Corresponding author. Tel.: +81 75 753 4545; fax: +81 75 753 4575.
E-mail address: hashidam@pharm.kyoto-u.ac.jp (M. Hashida).

0142-9612/$ - see front matter © 2006 Elsevier Ltd. All rights reserved.
doi:10.1016/j.biomaterials.2006.08.045

novel fucosylated lipid, cholesten-5-yloxy-*N*-{4-[(1-imino-2-L-thiofucosyl-ethyl)-amino] butyl}formamide (Fuc-C4-Chol), which poses fucose as a ligand for receptor recognition, a cholesterol derivative for stable insertion into liposomes and carrying a positive charge [18]. Therefore, fucosylated cationic liposomes (Fuc-liposomes) with a high density of fucose and a positive charge on the surface of liposomes containing more Fuc-C4-Chol, could achieve better Kupffer cell-selective delivery of NFκB decoy. Moreover, considering that the site of action of NFκB decoy is the cytoplasm, we chose dioleoylphosphatidylethanolamine (DOPE), which helps the gene to escape from endosomes through a conformational change at low pH [19].

The purpose of this work was to develop Kupffer selective targeting of NFκB decoy to Kupffer cells after intravenous injection. We prepared Fuc-liposome using Fuc-C4-Chol and investigated the distribution of Fuc-liposomes/NFκB decoy complexes after intravenous injection. The inhibitory effect of cytokine production by Fuc-liposomes/NFκB complexes was also examined. This is an initial report of the Kupffer cell-selective delivery of NFκB decoy and its therapeutic effect using Fuc-liposomes given by intravenous injection.

2. Material and methods

2.1. Materials

N-(4-aminoethyl) carbamic acid tert-butyl erter was purchased from Tokyo Kasei Kogyo Co. Ltd. (Tokyo, Japan). DOPE was purchased from Avanti Polar Lipids Inc. (Alabaster, AL, USA). Cholesteryl chloroformate, heparin and collagenase and D-(+)-galactosamine were purchased from Sigma Chemicals Pvt. Ltd. (St Louis, MO, USA). Oligonucleotides (NFκB decoy: 5′-AGTTGAGGGGACTTTCCCAGGC-3′, 5′-GCCT GGGAAAGTCCCCTCAACT-3′, random decoy: 5′-TTGCCGTACCT GACTTAGCC-3′, 5′-GGCTAAGTCAGGTACGGCAA-3′) were purchased from Operon Biotechnologies Inc. (Tokyo, Japan). L-(−)-Fucose, ethylene glycol-*bis* (*b*-aminoethylether)-*N,N,N′,N′*-tetraacetic acid (EGTA), Clear-Sol I and cholesterol were purchased from Nacalai Tesque Inc. (Kyoto, Japan). MEGALABEL™ 5′-End Labeling Kit was purchased from Takara Bio Inc. (Shiga, Japan). Soluene-350 was purchased from Perkin Elmer Inc. (Boston, MA, USA). An NAP-5 column was purchased from Amersham Biosciences Co. (Piscatway, NJ, USA). Trypan blue was purchased from Invitrogen Co. (Grand Island, NY, USA). Mouse TNFα BD OptEIA™ ELISA Kit was purchased from Becton, Dickinson and Company (Mississauga, Canada). Fraction-PREP™ Nuclear/Cytosol Fraction Kit was purchased from BioVision Inc. (Mountain View, CA, USA). Chemiluminescent NFκB Activation Assay Kit was purchased from Oxford Biomedical Research Inc. (Oxford, MI, USA). D-(+)-mannose and transaminase CII test Wako were purchased from Wako Pure Chemical Industries Ltd. (Osaka, Japan).

2.2. Animals

Female ICR mice (5-week old, 22–24 g) and female C57BL/6 mice (6-week old, 18–20 g) were obtained from Shizuoka Agricultural Co-operative Association for Laboratory Animals (Shizuoka, Japan). All animal experiments were carried out in accordance with the Principles of Laboratory Animal Care as adopted and promulgated by the US National Institutes of Health and with the Guidelines for Animal Experiments of Kyoto University.

2.3. Radiophosphorylation of decoy oligonucleotides

Annealed NFκB decoy was labeled with [γ-^{32}P] ATP using MEGALABEL™ 5′-End Labeling Kit with some modification as reported previously [11]. Briefly, oligonucleotides, [γ-^{32}P] ATP and T4 polynucleotide kinase were mixed in phosphorylation buffer. After a 30-min incubation at 37 °C, the mixture was incubated for 10 min at 70 °C in order to inactivate T4 polynucleotide kinase. Then, the mixture was purified by gel chromatography using a NAP 5 column and eluted with 10 mM Tris–Cl and 1 mM EDTA (pH 8.0). The fractions containing the derivatives were selected based on their radioactivity.

2.4. Synthesis of Fuc-C4-Chol

Fuc-C4-Chol was synthesized as reported previously [18,20]. Briefly, cholesteryl chloroformate and *N*-(4-aminobutyl)carbamic acid *tert*-butyl ester were reacted in chloroform for 24 h at room temperature. A solution of trifluoroacetic acid and chloroform was added dropwise and the mixture was stirred for 4 h at 4 °C. The solvent was evaporated to obtain *N*-(4-aminobutyl)-(cholesten-5-yloxyl)formamide which was then combined with 2-imino-2-methoxyethyl-1-thiofucoside and the mixture was stirred for 24 h at room temperature. After evaporation, the resultant material was suspended in water, dialyzed against distilled water for 48 h (12 kDa cut-off dialysis tubing), and then lyophilized. Man-C4-Chol and Gal-C4-Chol were synthesized in the similar manner using mannose or galactose.

2.5. Preparation of liposomes and their complex with NFκB decoy

Fuc-C4-Chol was mixed with DOPE in chloroform at a molar ratio of 3:2 and the mixture was dried, vacuum desiccated and resuspended in sterile 5% dextrose. After hydration for 30 min at room temperature, the dispersion was sonicated for 10 min in a bath sonicator and then for 3 min in a tip sonicator to form liposomes. The particle size of the liposomes and liposomes/NFκB decoy complexes were measured using dynamic light scattering spectrophotometer (LS-900, Otsuka Electronics, Osaka, Japan). The zeta potential of liposomes and liposome/NFκB decoy complexes were measured by Nano ZS (Malvern Instruments Ltd., Malvern, WR, UK). The preparation of liposomes/NFκB decoy complexes for in vivo use was carried out by the method of Kawakami et al. [13]. Equal volumes of NFκB decoy and stock liposome solution were diluted with 5% dextrose at room temperature. Then, the NFκB decoy solution was added rapidly to the liposome solution and the mixture was agitated rapidly by pumping it up and down twice in the pipet tip. The mixture was then left at room temperature for 30 min. The theoretical charge ratio of lipid/NFκB decoy was calculated as a molar ratio of Fuc-C4-Chol (monovalent) to a nucleotide unit (average molecular weight 330) [21]. Man-liposomes and Gal-liposomes were prepared in the similar manner.

2.6. In vivo distribution

The in vivo distribution was examined as previously reported [22]. Fuc-liposomes/NFκB decoy complexes in 300 μl 5% dextrose solution were intravenously injected into mice. Blood was collected from the vena cava at 1, 3, 10, 30 and 60 min, and mice were killed at each collection time point. Liver, kidney, spleen, heart and lung were removed, washed with saline, blotted dry and weighed. Immediately prior to blood collection, urine was also collected directly from the urinary bladder. Ten μl blood and 200 μl urine, and a small amount of each tissue were digested with Soluene-350 (0.7 ml for blood, urine and tissues) by incubation overnight at 54 °C. Following digestion, 0.2 ml isopropanol, 0.2 ml 30% hydroxyperoxide, 0.1 ml 5 M HCl, and 5.0 ml Clear-Sol I were added. The samples were stored overnight, and radioactivity was measured in a scintillation counter (LSA-500, Beckman, Tokyo, Japan).

2.7. Intrahepatic distribution

The intrahepatic distribution of Fuc-liposomes/[^{32}P] NFκB decoy complexes was determined as in our previous report [18]. Five minutes after intravenous injection of NFκB decoy or Fuc-liposomes/[^{32}P] NFκB decoy complexes, each mouse was anesthetized with diethyl ether and the liver was perfused with pre-perfusion buffer (Ca^{2+}, Mg^{2+}-free Hanks buffer, pH 7.4 containing 1000 units/L heparin and 0.19 g/L EGTA) for 6 min at 5 ml/min followed by Hanks buffer containing 5 mM $CaCl_2$ and 220 units/ml collagenase (Type I) (pH 7.4) for 6 min at 5 ml/min. After discontinuation of the perfusion, the liver was removed and the liver cells were dispersed in ice-cold Hanks-HEPES buffer. The cell suspension was filtered through cotton gauze, followed by centrifugation at 50*g* for 1 min at 4 °C. The pellet containing parenchymal cells (PC) was washed four times with ice-cold Hanks-HEPES buffer. The supernatant containing NPC was collected and purified by centrifugation at 50*g* for 1 min at 4 °C (four times). PC and NPC suspensions were centrifuged at 340*g* for 10 min. PC and NPC were then resuspended separately in ice-cold Hanks-HEPES buffer (final volume 2 ml). The cell number and viability were determined by the trypan blue exclusion method. The radioactivity of 500 μl of each cell suspension was measured by the same method as for the in vivo distribution. To investigate the contribution of Kupffer cells on liver accumulation of Fuc-liposome/NFκB decoy complex, mice were pretreated with $GdCl_3$ (30 mg/kg) 24 h before experiment.

2.8. Animal treatment protocol

For cytokine secretion assessment, blood was collected from ICR mice 1 h for TNFα, 6 h for IFNγ after intravenous injection of LPS (0.4 mg/kg). The blood was allowed to coagulate for 2–3 h at 4 °C and serum was isolated as the supernatant fraction following centrifugation at 2000*g* for 20 min. The serum samples were immediately stored at −80 °C. The amounts of TNFα and IFNγ were analyzed using an OptiEIA™ ELISA Kit according to the manufacturer's protocol. For severe liver injury model, C57BL/6 mice were injected intraperitoneally with LPS (0.05 mg/kg) and D-galactosamine (1000 mg/kg) in pyrogen-free saline. The blood was collected from mice 3 h after LPS and D-galactosamine treatment. The blood was allowed to coagulate for 2–3 h at 4 °C and serum was isolated as the supernatant fraction following centrifugation at 2000*g* for 20 min. Serum ALT and AST were measured with transaminase C II test Wako according to the manufacturer's protocol.

2.9. Enzyme immunoassay (EIA) for nuclear NFκB measurement

Liver was removed, washed with ice-cold saline and blotted dry. A small amount of liver was homogenized in phosphate-buffered saline. Pellets of cells were obtained by centrifugation at 500*g* for 2 min, and a nuclear extract was prepared using a Nuclear/Cytosol Fraction Kit. The amounts of NFκB in the nuclei were measured with an NFκB Activation Assay Kit according to the manufacturer's protocol.

2.10. Statistical analyses

Statistical comparisons were performed by Student's *t*-test for two groups and one-way ANOVA for multiple groups. Post hoc multiple comparisons were made by using Tukey's test.

3. Results

3.1. Particle size and zeta potential of Fuc-liposomes and their complex with NFκB decoy

The mean diameter and zeta potential of Fuc-liposomes or Fuc-liposomes/NFκB decoy complexes in 5% dextrose were mesured. The mean diameter of the Fuc-liposomes and Fuc-liposomes/NFκB decoy complexes were 79.5 ± 1.45 nm ($n = 3$) and 64.5 ± 1.84 nm ($n = 3$), respectively. After forming complexes with NFκB decoy, the charge on the surface of the Fuc-liposomes/NFκB decoy complexes was reduced to 37.4 ± 2.84 nm ($n = 3$) compared with Fuc-liposomes (62.0 ± 0.91 nm, $n = 3$) but still slightly cationic.

3.2. Rapid and high liver accumulation of Fuc-liposome/NFκB decoy complexes

Fig. 1 shows the time-courses of the radioactivity in blood, spleen, liver and kidney after intravenous injection of naked [^{32}P] NFκB decoy or Fuc-liposomes/[^{32}P] NFκB decoy complex. High and rapid liver accumulation of the Fuc-liposome/[^{32}P] NFκB decoy complex was observed. Following liver accumulation, the Fuc-liposome/[^{32}P]

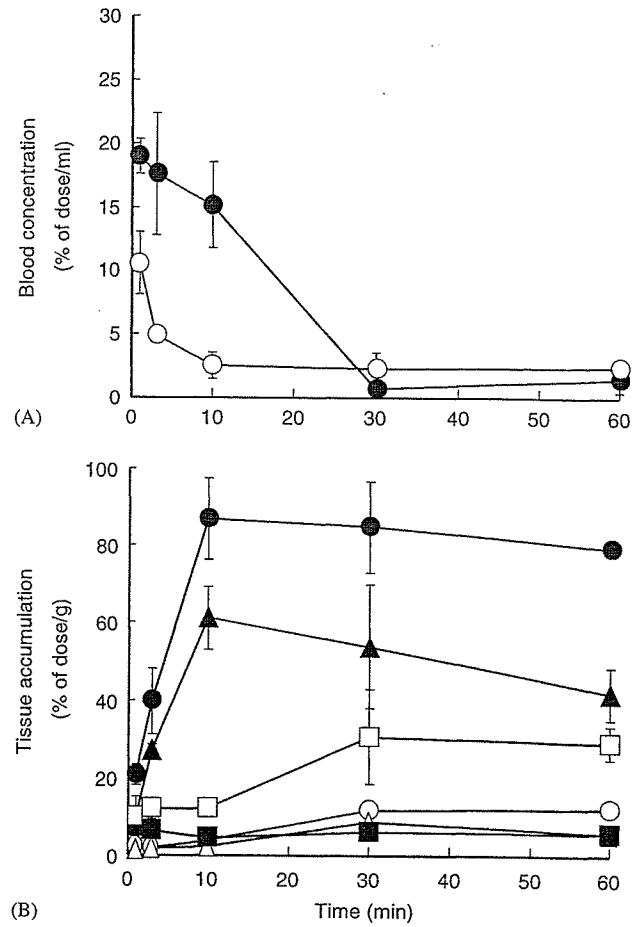

Fig. 1. Blood concentration of [^{32}P] naked NFκB decoy (○) and Fuc-liposome/[^{32}P] NFκB decoy complex (●) (A) and tissue accumulation of [^{32}P] naked NFκB decoy (liver ○, spleen △, kidney □) and Fuc-liposome/[^{32}P] NFκB decoy complex (liver ●, spleen ▲, kidney ■) after intravenous injection into mice (B). [^{32}P] NFκB decoy (NFκB decoy 20 μg/mouse) was complexed with Fuc-liposomes at a charge ratio of 1.0:2.3 (−:+). Radioactivity was determined in blood, liver, lung and spleen after 1, 3, 10, 30 and 60 min.